

## Performance of Chopper Spectrometers

M. Arai<sup>1</sup>, A.D. Taylor<sup>2</sup>, S.M. Bennington<sup>2</sup>, Z.A. Bowden<sup>2</sup>, R. Osborn<sup>2</sup>, M. Kohgi<sup>3</sup>, K. Ohoyama<sup>3</sup> and T. Nakane<sup>4</sup>

<sup>1</sup>National Laboratory for High Energy Physics, Oho, Tsukuba 305 Japan

<sup>2</sup>Rutherford Appleton Laboratory, Chilton, Didcot, Oxon OX11 0QX, UK

<sup>3</sup>Tohoku University, Aoba, Aoba-ku, Sendai 980, Japan

<sup>4</sup>Matel. Res. Inst., Tohoku University, Katahira, Aoba-ku, Sendai 980, Japan

### ABSTRACT

We discuss the performance of chopper spectrometers at pulsed neutron sources, with particular reference to results from MARI, HET and INC. Finally we suggest optimized parameters for several options on the performance.

### 1. Introduction

#### 1.1. The Standard Spectrometer for a Pulsed Neutron Source

In a direct geometry spectrometer on a pulsed neutron source the incident neutron energy is monochromatized by a mechanical fermi chopper phased to the source. This is the natural type of spectrometer for inelastic scattering on a pulse neutron source. The wide dynamical range in Q-E space gives a unique opportunity for new science as we have shown in another report in this volume<sup>1</sup>).

The overall performance of a chopper spectrometer on a pulsed neutron source requires the optimization of many aspects of its performance -- intensity, resolution, background, angular coverage, dynamic range etc. -- within the constraints imposed by the nature of the source (current, frequency etc.), the target/moderator system (material, coupling, geometry etc.), the beam line components available and the source geometry.

At present HET and MARI at the ISIS facility of Rutherford Appleton Laboratory in UK, LRMECS and HRMECS at the IPNS facility of Argonne National Laboratory in USA and INC at the KENS facility of National Laboratory for High Energy Physics in Japan are fully operational. The design parameters for these spectrometers are summarized in Table I. In this report we will give an overview of the performance of these spectrometers and concentrate on HET, MARI and INC, which have almost identical chopper systems, to discuss practical aspects of their performance and problems. We also give some suggestions for future optimizations.

|        | Proton Current ( $\mu$ A) | Moderator Target factor | Flux at moderator (n/eV.sr.100cm <sup>2</sup> .s) | Moderator Area (*100cm <sup>2</sup> ) | Chopper Transmiss | L1+L3 (cm) | Scattering Angle             | L2 (cm)           | $\Delta E/E$ | Intensity at Sample (n/cm <sup>2</sup> .s) | Int/ $\Delta\Omega$ (Counting rate) | Normalized by MARI   |
|--------|---------------------------|-------------------------|---|---------------------------------------|-------------------|------------|------------------------------|-------------------|--------------|--|-------------------------------------|----------------------|
| MARI   | 100                       | 1                       | 3.00E+12  | 0.64                                  | 0.8               | 1170       | 3°-135°                      | 400               | 1.0%         | 2244                                       | 1.40                                | 1.00                 |
| HET    | 100                       | 1                       | 3.60E+12  | 0.64                                  | 0.8               | 1170       | 3°-7°<br>9°-29°<br>134°-136° | 400<br>250<br>400 | 1.0%         | 2693                                       | 1.68<br>4.31<br>1.68                | 1.20<br>3.07<br>1.20 |
| INC    | 3                         | 2                       | 2.16E+11  | 0.64                                  | 0.8               | 820        | 5°-40°<br>40°-130°           | 250<br>130        | 1.5%         | 493  | 0.79<br>2.92                        | 0.56<br>2.08         |
| LRMECS | 14                        | 2                       | 1.01E+12  | 0.64                                  | 0.8               | 683        | 3°-120°                      | 250               | 2.0%         | 4425                                       | 7.08                                | 5.05                 |
| HRMECS | 14                        | 2                       | 1.01E+12  | 0.64                                  | 0.8               | 1985       | 3°~                          | 400               | 1.0%         | 538  | 0.34                                | 0.20                 |

Table I Current performance of chopper spectrometers. The calculation is for epithermal region.  
 Intensity at Sample = Flux.Moderator.Area\*Chop.Trans\* $\Delta E/(L1+L3)^2$   
 Int/ $\Delta\Omega$  = Intensity at Sample / L2<sup>2</sup>

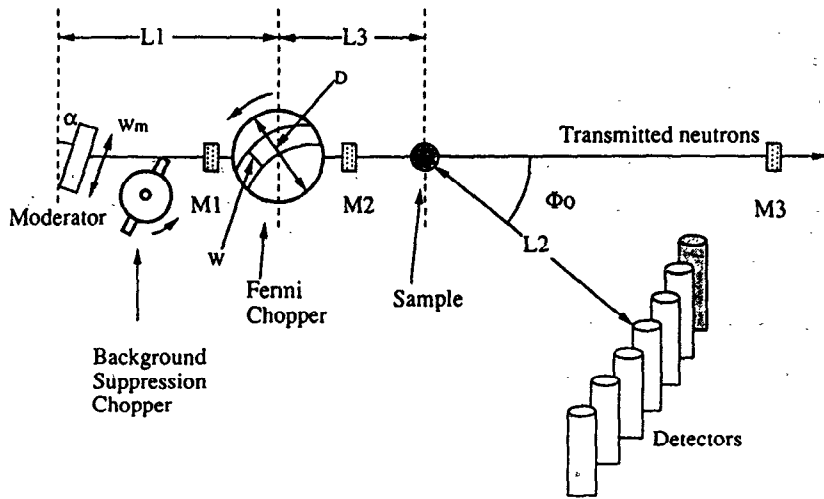


Fig. 1 Schematic diagram of a chopper spectrometer.

## 1.2. Outline of a Chopper Spectrometer

The structure of a chopper spectrometer is shown in Fig.1. Neutrons starting at time  $t_0$  at a moderator are monochromatized by a fermi chopper at distance  $L_1$  which is phased to the neutron burst time. Fast neutrons are cut out by a background suppression chopper at an upstream position. The incident neutron spectrum is monitored by  $M_1$ , the monochromatized spectrum by  $M_2$  and the transmitted spectrum by  $M_3$ . As the only moving components in the spectrometer are the choppers, enormous detector arrays can be easily arranged around the sample covering a wide range of scattering angles.

## 2. Energy Resolution

### 2.1. Conventional Expression for the Resolution

The resolution depends on the time width of the moderator pulse  $\Delta t_m$ , the time width of the chopper opening  $\Delta t_{ch}$  and the flight path lengths  $L_1, L_2$  and  $L_3$ . A detailed derivation of the monochromatized pulse shape is given fully in reference (2). However it is quite helpful to illustrate the essence of the resolution for the present discussion.

The asymmetric moderator pulse shape can be described by a slowing down and storage component<sup>3</sup>). Propagating neutrons are transmitted through the chopper, when the energy (the slope in the Time-Length diagram in Fig. 2 is appropriate for the chopper opening at  $L_1$ . The chopper opening time width is very short ( typically a few  $\mu s$  ), giving a pin-hole camera effect in the time-length space. This reverses the image of the moderator pulse shape at the detecting point.

The actual pulse shape is obtained by the velocity integration of the various neutron energies which pass through the chopper. The calculation is achieved by a convolution of the moderator pulse function and chopper opening function. However in most cases the following equation<sup>4,5</sup>) gives a reasonable estimate for the energy and momentum resolution especially in the slowing down region above the Maxwellian.

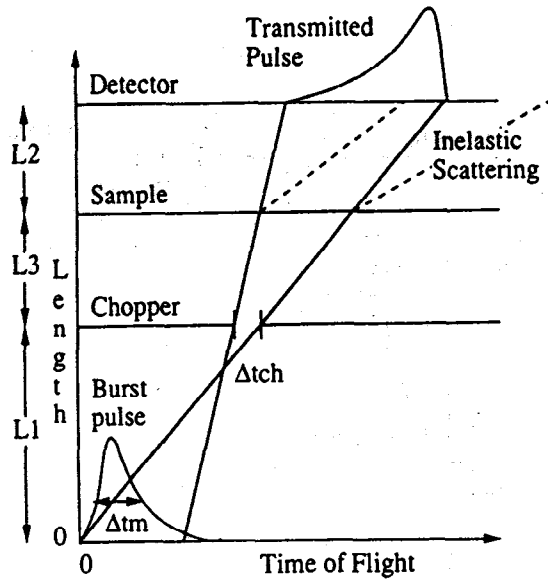


Fig. 2 Pin-hole camera effect on the pulse shape in time-length space.

$$\frac{\Delta \epsilon}{E_i} = \left[ \left\{ 2R_1 \left[ 1 + \frac{L_1 + L_3}{L_2} \left( 1 - \frac{\epsilon}{E_i} \right)^{3/2} \right] \right\}^2 + \left\{ 2R_2 \left[ 1 + \frac{L_3}{L_2} \left( 1 - \frac{\epsilon}{E_i} \right)^{3/2} \right] \right\}^2 \right]^{1/2} \quad (1)$$

$$\frac{\Delta Q}{Q} = \frac{2mE_i}{h^2 Q^2} \left\{ \frac{E_i}{4E_f} (\cos(\Phi_0) - \sqrt{\frac{E_f}{E_i}})^2 \left( \frac{\Delta \epsilon}{E_i} \right)^2 + \frac{E_f}{E_i} \sin^2(\Phi_0) \Delta \Phi^2 \right\}^{1/2} \quad (2)$$

where  $R_1 = \Delta t_{ch}/t_{ch}$ ,  $R_2 = \Delta t_m/t_{ch}$

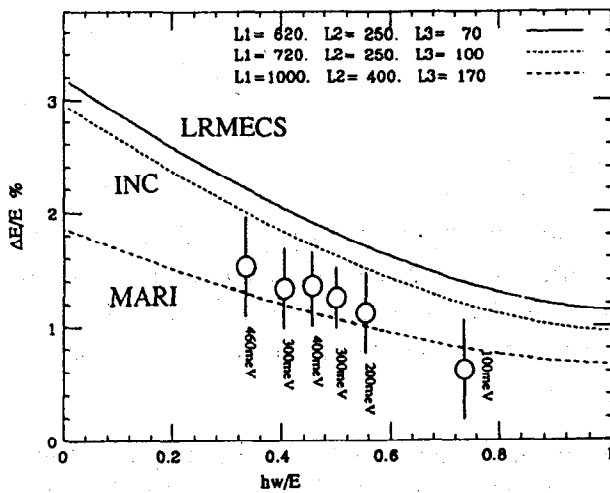


Fig. 3 Calculated energy resolution from eq. (1). Circles are the observation.

## 2.2. Moderator Characteristics and Time Structure

The moderator characteristics are very important for the performance of a spectrometer at a pulsed neutron source. The time structure of the moderator pulse is directly reflected in the resolution of the spectrometer. The calculated time widths for several moderators are shown in Fig. 4 6). The deviation from the straight line described by  $\Delta t_m [\mu s] \sim 1.8 \sqrt{E [eV]}$  reflects the contribution of the storage

The moderator time width is described approximately by  $\Delta t_m [\mu s] \sim 1.8 \sqrt{E [eV]}$  in the slowing down region. For resolution matching, the chopper opening time  $\Delta t_{ch}$  should be matched to the  $\Delta t_m$ . The length  $L_1$  and  $L_2$  are the dominant components for the overall energy resolution. Figure 3 shows the calculated energy resolution of the LRMECS, INC and MARI spectrometers.

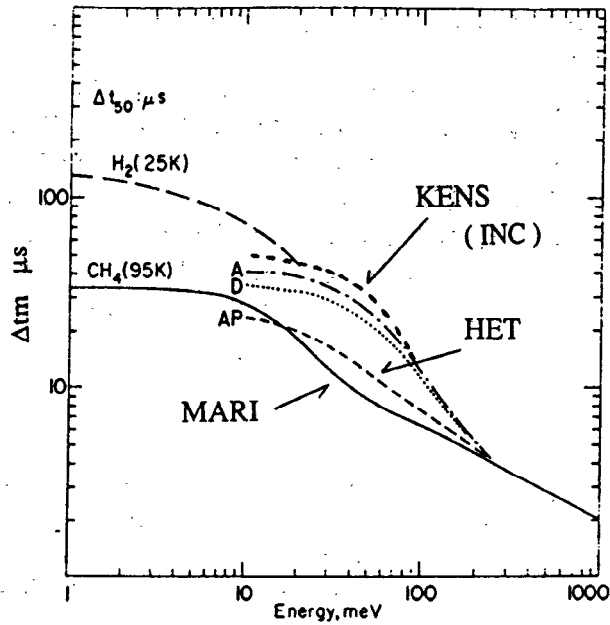


Fig. 4 Predicted FWHM of the moderator pulse shape as a function of energy.

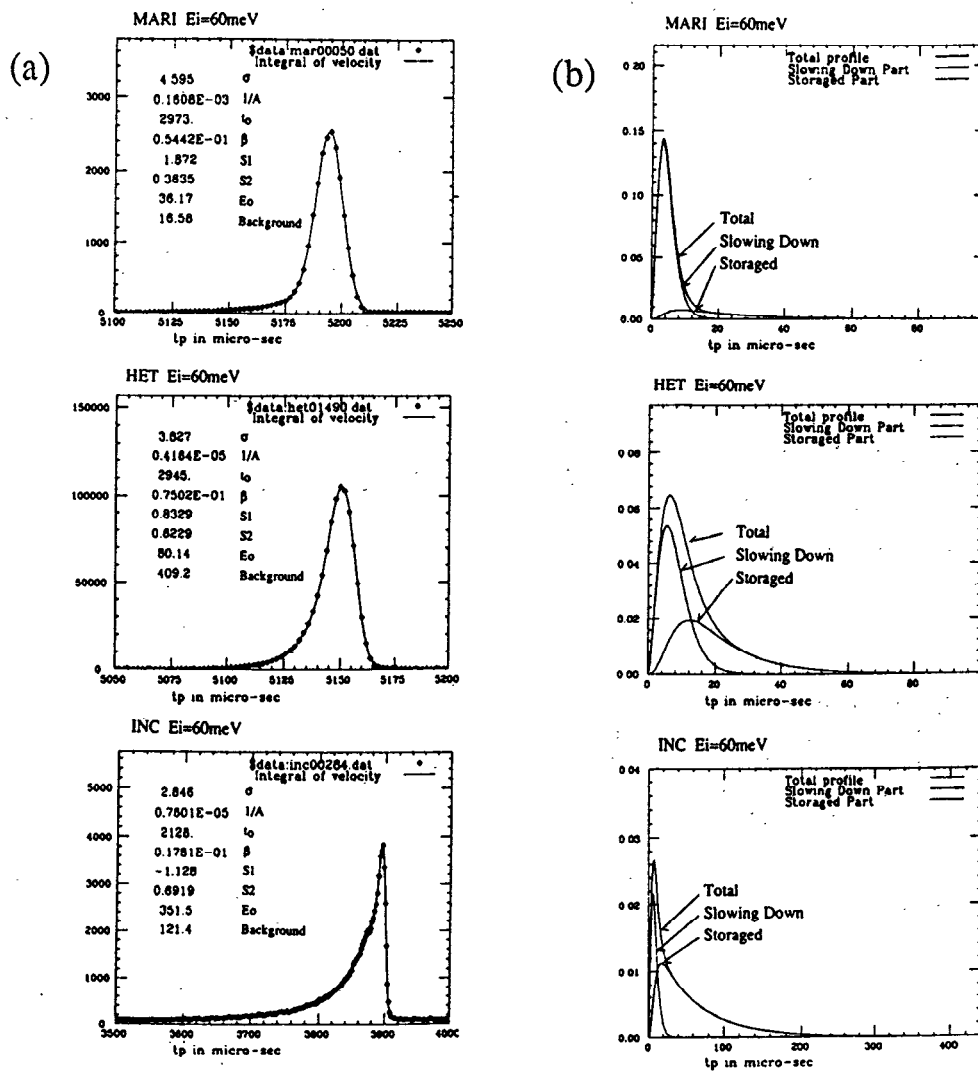


Fig. 5 (a) Transmitted pulse shape at the downstream monitor M3 for  $E_i=60\text{meV}$ . The line is a fit.  $\sigma$ , chopper opening time width; A, amplitude, other parameter's notation is the same as ref.3). (b) Expected moderator pulse shape at the moderator surface.

component. A poisoned or cooled moderator maintains good resolution in the low energy region by sacrificing some intensity.

Here we estimated the moderator pulse shape from the observed pulse shape at the downstream monitor M<sub>3</sub> shown in Fig. 5 (a). A deconvolution with a chopper window function (similar to a Gaussian) gives us a rough estimate of the moderator characteristics as shown in Fig. 5 (b). The MARI moderator is liquid CH<sub>4</sub> at 100K poisoned at 2.25cm depth. The HET moderator is ambient H<sub>2</sub>O poisoned at 1.5cm depth. The INC moderator is ambient non-poisoned H<sub>2</sub>O. The difference in poisoning has an enormous effect on the pulse shape and the resolution of the spectrometer.

### 2.3. Observed Resolution

In the epithermal region, the moderator pulse shape is dominated by the slowing down component. The pulse shape is close to symmetric so the observed pulsed shape gives a direct measure of the resolution of a spectrometer. Fig. 6 (a) shows the observation of spin waves in the one dimensional antiferromagnet KFeS<sub>2</sub> on MARI and the estimated energy resolution is plotted as circles in Fig. 3. The agreement between the observation and the calculation is good for various incident energies and we can see that the simple resolution equation (1) gives us a reasonable estimate of the resolution.

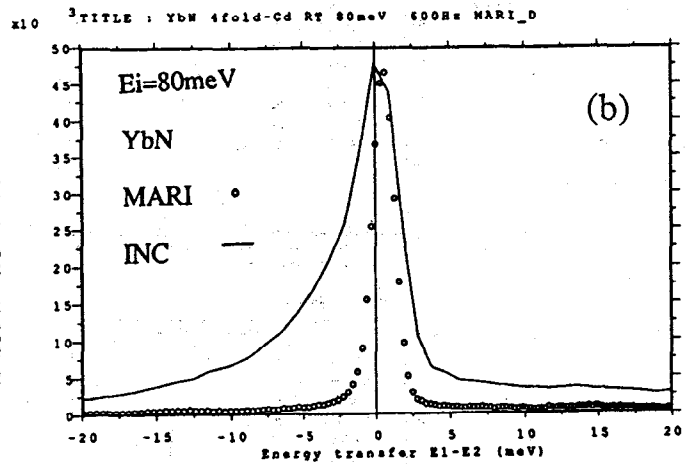
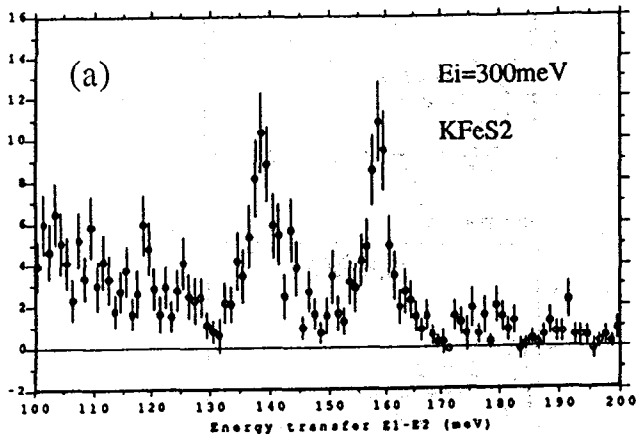
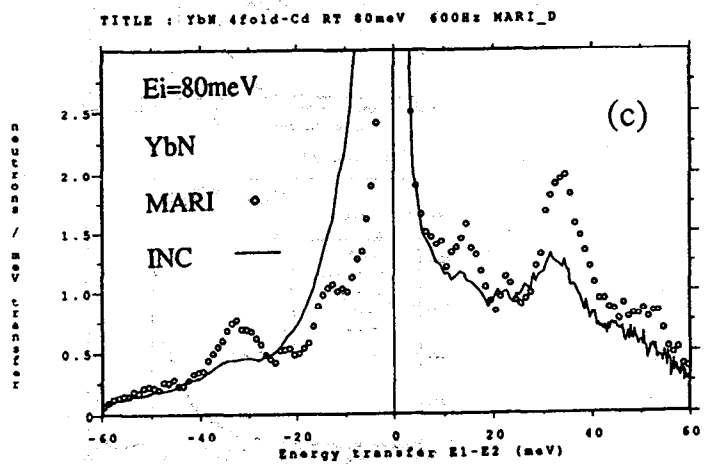


Fig. 6 (a) Spin wave excitation peak of 1D-antiferromagnet KFeS<sub>2</sub> with  $E_i=300\text{meV}$ . (b) Comparison of the energy resolution at the elastic peak for  $E_i=80\text{meV}$  measured on YbN. Intensity was normalized at the peak. (c) Comparison at the inelastic region on YbN  $E_i=80\text{meV}$ . Intensity is normalized per detector solid angle.



When the incident energy is lower than the epithermal-Maxwellian cross-over energy, the storage component becomes the dominant part, and the moderator pulse

width increases rapidly as seen in Fig. 4. This effect is clearly shown in Fig. 6 (b) and (c) observed on the crystal field excitation of YbN with the incident energy of 80meV. The energy resolution is three times worse for INC than MARI at this energy, although only 50% worse at epithermal region.

The need for good resolution is illustrated by problems taken from the both extremes of these instruments energy range. At the low energy end, Fig. 7 (a) shows the spectrum of Tm:YBa<sub>2</sub>Cu<sub>3</sub>O<sub>7</sub> taken with E<sub>i</sub>=20meV on MARI. The line width of the crystal field excitations was followed using the FWHM resolution of about 300μeV - with a 80μeV leading edge ! At high energy, HET required the 50meV resolution available at 2.14eV to observe the full inter-multiplet spectrum of Tm up to 1776meV, Fig. 7 (b). This high resolution has been crucial in enabling a wide range of science to be tackled by these spectrometers.

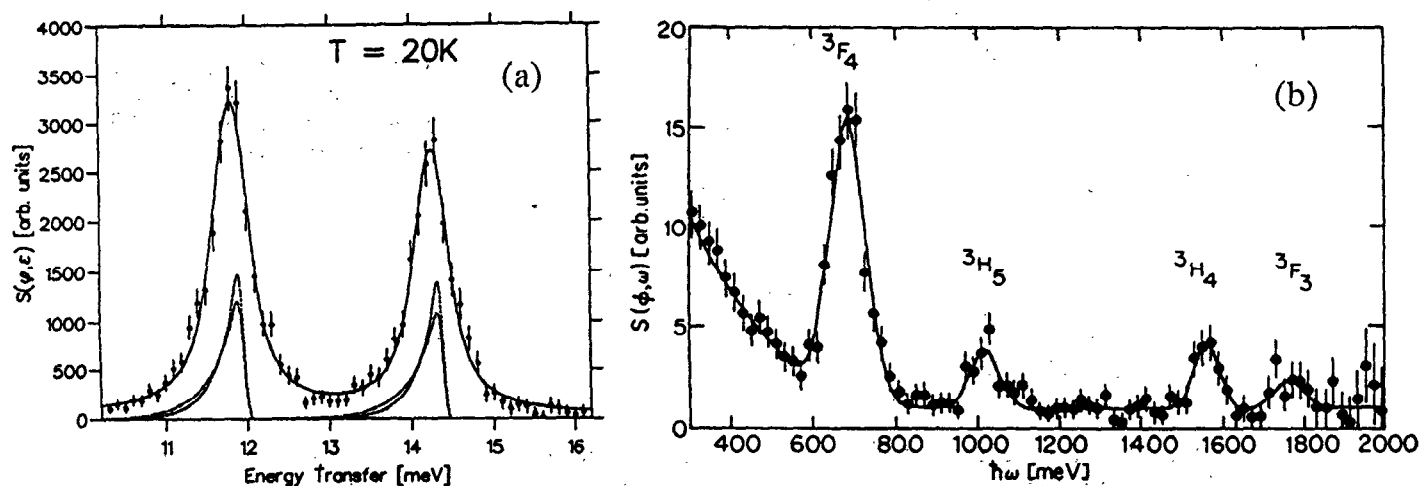


Fig. 7 (a) Measurement on Tm:YBa<sub>2</sub>Cu<sub>3</sub>O<sub>7</sub> with E<sub>i</sub>=20meV on MARI. (b) Measurement on Tm with E<sub>i</sub>=2140meV on HET.

### 3. Intensity

From a practical point of view we should design a spectrometer to have reasonable intensity at the sample position. In Table I we estimated the neutron flux at the sample position from the calculated neutron flux at the moderator surface  $\Phi_0(E)^6$ , the moderator area M, chopper transmission T, flight path length L<sub>1</sub>, L<sub>2</sub> and L<sub>3</sub> and the designed resolution  $\Delta E$ . We obtain a value at the sample position close to observation for HET, MARI and INC by using the following equation<sup>5</sup>.

$$\text{Intensity at sample}(E) = \Phi_0(E) * M * T * \Delta E / (L_1 + L_3)^2 \quad (3)$$

The flux at the sample is more or less similar among the spectrometers (several thousands neutrons/cm<sup>2</sup>/s). This value is one order of magnitude smaller than that of the typical inelastic instrument in ILL. However a large number of detectors surrounding the sample can compensate the counting rate and provide one-day experiments as a typical measurement. The flux at the sample can be rapidly increased by a small relaxation in the energy resolution, so the optimization of the spectrometer performance is important. For example INC has 50% worse resolution than that of MARI. However the estimated counting rate per solid angle is only 50%

of that of MARI in spite of the large difference in proton current (30 times). This was confirmed by the measurement on YbN as shown in Fig. 6 (c).

#### 4. Angular Coverage

Chopper spectrometers naturally lend themselves to wide angular coverage. The only difficulty is the cost of detectors! In Fig. 8 we show the observable Q-E space for these spectrometers. HET has a very limited angular coverage both at the small ( $3^\circ \sim 7^\circ$ ) and the high angle ( $134^\circ \sim 136^\circ$ ), whereas MARI ( $3^\circ \sim 135^\circ$ ), INC ( $5^\circ \sim 130^\circ$ ) and LRMECS ( $3^\circ \sim 120^\circ$ ) have a very wide angle coverage. An important feature of MARI and LRMECS is their equi-resolution over the angular range. INC has

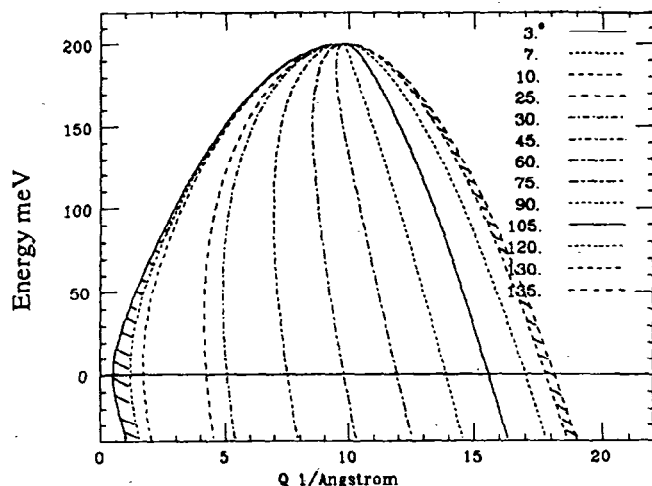


Fig. 8 Accessible Q-E space for  $E_i=200\text{meV}$ . The shaded area is for the HET 4m detector bank.

heterogeneous resolution from  $40^\circ$  to  $135^\circ$ . The wide angular coverage gives a full  $S(Q,E)$  measurement in one experiment, which is especially important to understand the dynamics and structure of non-crystalline materials. From our experience the equi-resolution angular coverage is very important in most experiments. Even when the scientific interest is concentrated at small angles as in magnetic scattering the phonon contribution can only be estimated from data at higher angles. If the energy resolution varied across the angular range this estimation would not work properly. Figure 9 shows the phonon contribution estimated from the high angle data under the magnetic scattering on  $\text{CeCu}_2\text{Si}_2$  on HET.

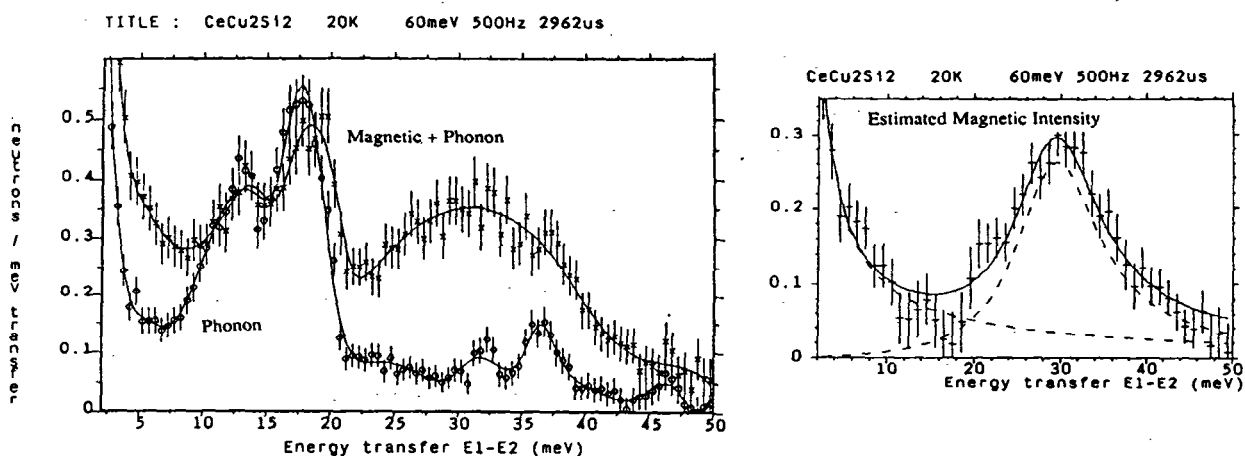


Fig. 9 Estimation of the magnetic scattering of  $\text{CeCu}_2\text{Si}_2$  at small angles after subtraction of the phonon contribution using high angle data.

## 5. Background

### 5.1. Delayed Neutron Background

There are contradictory requirements in the choice of target material. Fissile material such as uranium produces twice as many neutrons as a non-fissile target such as tungsten or tantalum. However the accompanied delayed neutron background causes a lot of trouble in the data analysis and sometimes reduces the data quality. Figure 10 shows the observed data on g-SiO<sub>2</sub> from MARI with Ta and U targets under otherwise identical conditions. Here the data are normalized to an accumulated proton current of 10mAhrs. The signal was twice as intense with the U-target, but the background level was 30 times higher. ( The background level for the Ta-target is about 0.1 count/min/detector. This value is close to the ideal intrinsic noise level for <sup>3</sup>He detectors. ) The background level depends on the fast neutron cross-section of the sample, so that a simple subtraction of the empty cell data is not appropriate.

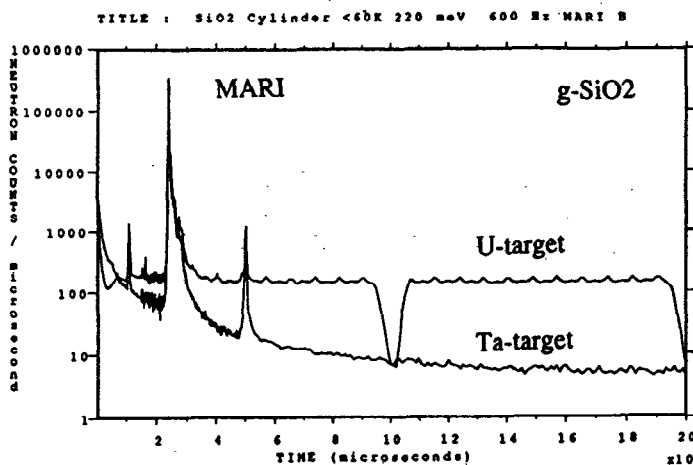


Fig. 10 Comparison of the background from g-SiO<sub>2</sub> on MARI with a U-target and Ta-target under otherwise identical conditions. The central dip for the U-target is due to the background suppression chopper.

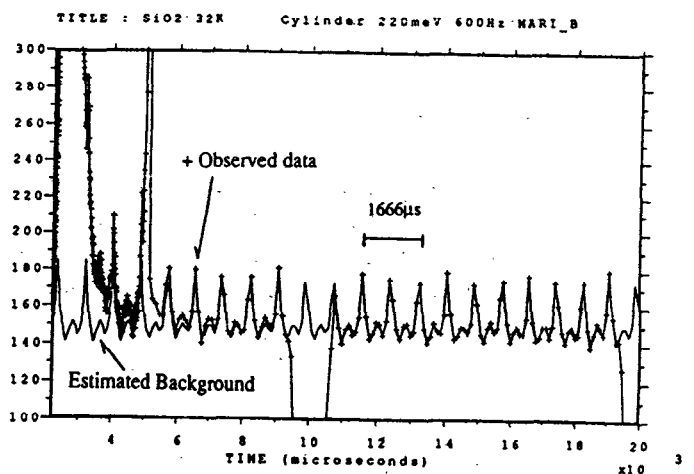


Fig. 11 Modulated delayed neutron background and estimated correction.

The modulated structure in the delayed neutron background depends on the chopper conditions such as frequency, phase and attenuating structure. Such a modulated background can be subtracted by averaging the long time background as shown in Fig.11. The background was averaged by folding the data in the long time region with the chopper periodicity of 1666.7μs (600Hz). The complete subtraction is difficult and sometimes the quality of low intensity data is diminished. The modulated background does not affect high energy excitation data, because the scattered intensity is concentrated in a small time-of-flight region. For low energy transfer measurements, however, the scattered intensity is spread over a wide range of time-of-flight and the signal can become comparable to the delayed neutron background. To some level we can diminish the delayed neutron background by a careful design of the collimator system. However since this background is a sample born background, it is difficult to avoid if we chose fissile material for the target.

In Fig.12 we compare the data for the same sample of YbN at MARI and INC. The signal-to-background (S/N) ratio is ten times worse in MARI. After taking into account the difference of the accelerator duty cycle (20Hz for INC and 50Hz for



MARI), the factor is still four, which may be attributable to differences of collimation system, or to reflector differences between KENS and ISIS.

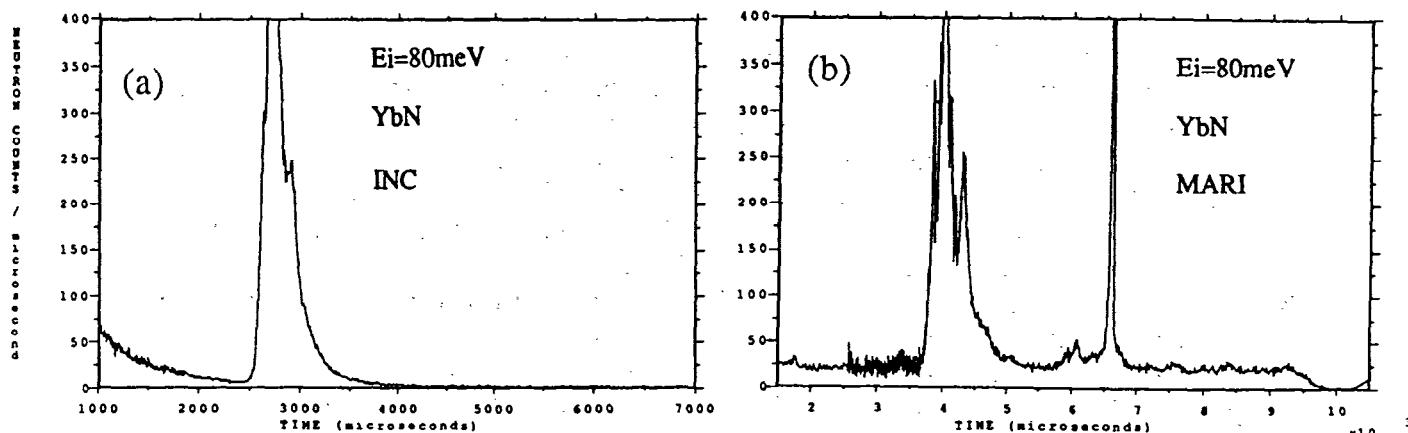


Fig. 12 Comparison of the data from the same sample of YbN for (a) INC and (b) MARI.

## 5.2. Background Suppression Chopper

A key device for these instruments is a background suppression chopper. HET and MARI are effective to energies over 2eV, whereas LRMECS, HRMECS and INC without a background suppression chopper are restricted to less than ~500meV due to the high background for many problems.

## 5.3. Spectrometer Born Background

Another background source is within the spectrometer itself where neutron can be scattered by internal components such as the sample cell, sample environment equipment, the vacuum chamber wall and the shielding around the sample itself. External background is normally broad in time (Fig. 11), whereas multiply scattered background from within the spectrometer can give very sharp and intense spurious peaks. Figure 13 shows an early measurement of the crystal field excitation of Tm:YBa<sub>2</sub>Cu<sub>3</sub>O<sub>7</sub> on MARI. The two peaks at higher energy transfer in Fig. 13 are the real excitation spectrum as shown in Fig. 7 (a). The first peak is spurious, produced by a multiple scattering from the flange of the cryostat above the sample. The elastic signal from the sample was further scattered by the flange and came to the detectors at a later time-of-flight, thus imitating an inelastic signal. Such processes are now suppressed by a strategically placed low albedo surface.

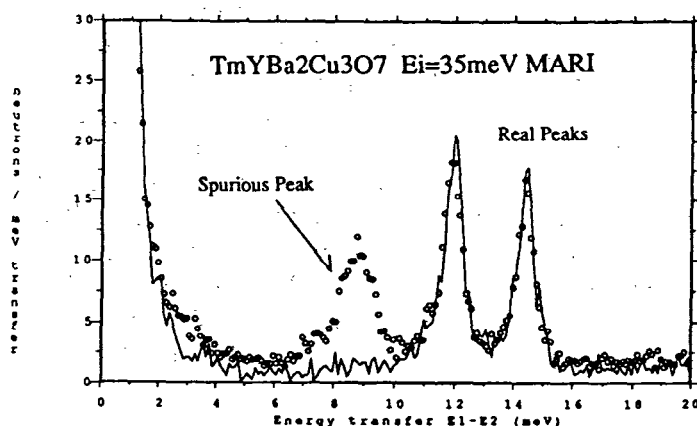


Fig. 13 Multiple scattering inside the spectrometer. The two peaks at higher energy transfer are the real excitations. The first peak is spurious.

A second example of internal background is coherent scattering from the thin aluminum membrane, situated downstream from the sample, which separates the spectrometer vacuum and sample vacuum. The baffle shields in the spectrometer shadow some detectors from this scattering but this is ineffective at the small angle region. The total flight path of this diffracted background is longer, again causing it to manifest itself as an apparent inelastic signal. It is present in an 'empty' spectrometer run, but sample attenuation make this effect difficult to estimate quantitatively.

## 6. Conclusion

There are no absolute criteria for the optimization of the performance of a chopper spectrometer, but the following rules of thumb are appropriate:

**Intensity:** It is important to obtain reasonable statistics in one day on a typical sample. On MARI 5000 n/cm<sup>2</sup>/s should satisfy this criterion for a wide variety of science. From this starting position we tried to find optimized parameters for chopper spectrometers at other neutron sources, subject to typical geometrical constraints, i.e.  $L_3/L_1=0.15$  and  $L_2/(L_1+L_3)=0.4$ .

In Table II, "High Resolution Option" corresponds to this condition. The last two columns show the expected intensity per unit solid angle normalized to that of MARI. By relaxing the resolution a little, we can achieve the similar statistics in spite of the considerably different proton current. In the "High Intensity Option" by relaxing the resolution by 50%, we can get 10 times higher intensity. The flux decreases proportionally to  $1/(\text{length})^3$  but the resolution is proportional to  $1/\text{length}$ . Therefore a careful design of the parameters can compensate the performance greatly.

**Angular Coverage:** Continuous angular coverage with equi-energy-resolution has been found to be practically very important. Even when the signal is concentrated at small angle, as with magnetic excitations, the high angle data with the same energy resolution is essential to estimate the non-magnetic contribution.

|  | Proton Current ( $\mu\text{A}$ ) | Moderator Factor | Flux at moderator (n/eV.sr.100cm <sup>2</sup> .s) | Moderator Area (*100cm <sup>2</sup> ) | Chopper Transmiss | L1 (cm) | L3 (cm) | L2 (cm) | $\Delta E/E$ | Intensity at Sample (n/cm <sup>2</sup> /s) | Int/ $\Delta\Omega$ | Local ratio normalized by MARI | Grand ratio normalized by MARI |
|--|----------------------------------|------------------|---|---------------------------------------|-------------------|---------|---------|---------|--------------|--|---------------------|--------------------------------|--------------------------------|
| <b>High Resolution Option ( for Maximum Proton Current and U-target)</b> |                                  |                  |   |                                       |                   |         |         |         |              |  |                     |                                |                                |
| MARI   | 200                              | 1                | 6.00E+12  | 0.64                                  | 0.8               | 969     | 145     | 388     | 1.0%         | 5000                                       | 3.33                | 1.00                           | 1.00                           |
| INC  | 8                                | 2                | 5.76E+11  | 0.64                                  | 0.8               | 663     | 99      | 265     | 1.5%         | 1500                                       | 2.13                | 0.64                           | 0.64                           |
| LRMECS   | 14                               | 2                | 1.01E+12  | 0.64                                  | 0.8               | 726     | 109     | 290     | 1.4%         | 2000                                       | 2.37                | 0.71                           | 0.71                           |
| <b>High intensity Option ( for Maximum Proton Current and U-target)</b>  |                                  |                  |   |                                       |                   |         |         |         |              |  |                     |                                |                                |
| MARI   | 200                              | 1                | 6.00E+12  | 0.64                                  | 0.8               | 611     | 92      | 244     | 1.6%         | 20000                                      | 33.51               | 1.00                           | 10.07                          |
| INC  | 8                                | 2                | 5.76E+11  | 0.64                                  | 0.8               | 444     | 67      | 178     | 2.3%         | 5000                                       | 15.85               | 0.47                           | 4.76                           |
| LRMECS   | 14                               | 2                | 1.01E+12  | 0.64                                  | 0.8               | 425     | 64      | 170     | 2.4%         | 10000                                      | 34.64               | 1.03                           | 10.41                          |
| <b>Low Background Option ( for non-fissile target )</b>                  |                                  |                  |   |                                       |                   |         |         |         |              |  |                     |                                |                                |
| MARI   | 200                              | 0.5              | 3.00E+12  | 0.64                                  | 0.8               | 829     | 124     | 331     | 1.2%         | 4000                                       | 3.64                | 1.00                           | 1.09                           |
| INC  | 8                                | 1                | 2.88E+11  | 0.64                                  | 0.8               | 584     | 88      | 233     | 1.7%         | 1100                                       | 2.02                | 0.55                           | 0.61                           |
| LRMECS   | 14                               | 0.5              | 2.52E+11  | 0.64                                  | 0.8               | 558     | 84      | 223     | 1.8%         | 1100                                       | 2.21                | 0.61                           | 0.66                           |

Table II Some optimizations of a spectrometer for several options.  
 Intensity at Sample (Ei) = Flux.Moderator.Area\*Chop.Trans\* $\Delta E/(L_1+L_3)^2$   
 Int/ $\Delta\Omega$  = Intensity at Sample / L2<sup>2</sup>. Constraint;  $L_3/L_1=0.15$  and  $L_2/(L_1+L_3)=0.4$

*Background:* The background level is often dominated by the target material. The delayed neutron background can be critical in a direct-geometry inelastic spectrometer, but on the other hand a fissile target actually provides twice the intensity for diffractometers and other instruments without increasing their background significantly. So the choice of the target material for a facility is difficult. The last calculation in Table II the "Low Background Option (for non-fissile targets)" suggests that we obtain intensity by relaxing the resolution by small amount. It may be worthwhile to consider this option for a high intensity spallation neutron source, where the optimization of the target-moderator coupling with a non-fissile target give the system with long life-time and good reliability.

## 7. Acknowledgement

The experiments on MARI were carried out during the commissioning period in 1991 under the UK-Japan collaboration on neutron scattering research. We are indebted to Prof. N. Watanabe for his continued support of this collaboration.

## References

- 1) A.D. Taylor et al., ICANS-XI MARI report.
- 2) C.-K. Loong, S. Ikeda and J.M. Carpenter, Nucl. Inst. Meth. Phys. Res. A260 (1987) 381
- 3) S. Ikeda and J.M. Carpenter, Nucl. Inst. Meth. Phys. Res. A239 (1985)536
- 4) C.J. Carlile, A.D. Taylor and W.G. Williams, Rutherford Appleton Laboratory Report, RAL-85-052
- 5) M. Arai, M. Kohgi, M. Itoh, H. Iwasa, N. watanabe, S. Ikeda and Y. Endoh, ICANS-X Proc. 297 (1988)
- 6) A.D. Taylor, Rutherford Appleton Laboratory Report, RAL-84-120, 1984

Q(R.Pynn): You mentioned many characteristics of spectrometers among which we have to choose in order to achieve total performance. Do you have any advice for us on how to make these choices?

A(A.D.Taylor): No. This is too hard a question to answer in general. However it is important not to be frozen into inaction by the large number of the options available. Your fourier analysis is, however, a helpful guide.